

**TAILORING NATURAL RUBBER/BUTADIENE RUBBER COMPOUNDS CONTAINING A
HYBRID CARBON BLACK-SILICA FILLER FOR AIRCRAFT TIRE TREADS:
THE EFFECT OF ZINC OXIDE AND DPG ADDITION SEQUENCE ON COMPOUND
PROPERTIES AND HYSTERESIS**

INDRIASARI^{1,2}, KAEWSAKUL, W.², NOORDERMEER, J.W.M.², DIERKES, W.K.² BLUME, A.²

¹ CENTER FOR MATERIAL TECHNOLOGY, AGENCY FOR THE ASSESSMENT AND APPLICATION OF TECHNOLOGY (BPPT), BUILDING 224, KAWASAN PUSPIPEK SERPONG, TANGERANG SELATAN, 15314, BANTEN, INDONESIA

² ELASTOMER TECHNOLOGY AND ENGINEERING, FACULTY OF ENGINEERING TECHNOLOGY, UNIVERSITY OF TWENTE, DRIENERLOLAAN 5, 7522NB ENSCHEDE, THE NETHERLANDS; I.INDRIASARI@UTWENTE.NL (I); W.KAEWSAKUL@UTWENTE.NL (W.K.); A.BLUME@UTWENTE.NL (A.B.); J.W.M.NOORDERMEER@UTWENTE.NL (J.W.M.N)

* Correspondence: w.k.dierkes@utwente.nl (W.K.D.); Tel.: +31-64-7682-000 (I.); +31-53-4894-721 (W.K.D.)

PRESENTED AT THE 196TH TECHNICAL MEETING
OF THE RUBBER DIVISION, ACS
CLEVELAND, OH, OCTOBER 8-10 2019

ISSN: 1547-1977

*ASTERISK IDENTIFIES SPEAKER/LEAD AUTHOR

TAILORING NATURAL RUBBER/BUTADIENE RUBBER COMPOUNDS CONTAINING A
HYBRID CARBON BLACK-SILICA FILLER FOR AIRCRAFT TIRE TREADS:
THE EFFECT OF ZINC OXIDE AND DPG ADDITION SEQUENCE ON COMPOUND
PROPERTIES AND HYSTERESIS

INDRIASARI^{1,2}, KAEWSAKUL, W.², NOORDERMEER, J.W.M.², DIERKES, W.K.² BLUME, A.²

¹ CENTER FOR MATERIAL TECHNOLOGY, AGENCY FOR THE ASSESSMENT AND APPLICATION OF TECHNOLOGY (BPPT), BUILDING 224, KAWASAN PUSPIPEK SERPONG, TANGERANG SELATAN, 15314, BANTEN, INDONESIA

² ELASTOMER TECHNOLOGY AND ENGINEERING, FACULTY OF ENGINEERING TECHNOLOGY, UNIVERSITY OF TWENTE, DRIENERLOLAAN 5, 7522NB ENSCHEDE, THE NETHERLANDS; I.INDRIASARI@UTWENTE.NL (I.);

W.KAEWSAKUL@UTWENTE.NL (W.K.); A.BLUME@UTWENTE.NL (A.B.); J.W.M.NOORDERMEER@UTWENTE.NL (J.W.M.N)

* Correspondence: w.k.dierkes@utwente.nl (W.K.D.); Tel.: +31-64-7682-000 (I.); +31-53-4894-721 (W.K.D.)

ABSTRACT

The properties needed for aircraft tire treads are significantly different from the ones required for passenger car or truck tires, for which improvements mainly focus on a better balance of rolling, wet skid and wear resistance. Aircraft tires experience severe operation conditions during service: The temperature can reach above the critical temperature of polymers, thus accelerating tread wear. To reduce the peak temperatures of the tire tread during departure and landing, the material of the tread should have a low hysteresis. Moreover, the tires need to be able to withstand high loads and impact during landing. Therefore they also require outstanding strength properties and reversion resistance.

This paper focuses on the influence of the processing sequence of ZnO and DPG on the properties mentioned above. It is based on a blend of natural and butadiene rubber reinforced with hybrid carbon black-silica fillers. From this study, we found that the ZnO addition sequence has a strong influence on the properties of rubber compounds, while the DPG addition sequence has almost no effect. The incorporation of ZnO in the first stage of mixing results in low Mooney viscosity, better silica dispersion, slow cure rate but high reversion resistance and high mechanical properties. When ZnO was omitted during the first stage of mixing and added in the last stage of mixing, it resulted in high filler-polymer interaction, which is beneficial for high stress-strain properties. However, the latter compounds were prone to reversion under prolonged vulcanization leading to a significant reduction of the modulus at 300% elongation and crosslink density. Finally, the addition sequence of ZnO and DPG does not influence the hysteresis.

The energy loss (hysteresis) of the compounds is influenced by the filler-filler and filler-polymer interaction as well as crosslink density. These properties vary with mixing procedure; i.e., adding ZnO in the first stage of mixing shows low filler-filler interaction but also low filler-polymer interaction, while adding ZnO in the last stage of mixing results in high Payne effect but also high filler-polymer interaction. In case of the degree of crosslinking, all compounds exhibit a similar level.

INTRODUCTION

Hysteresis, which reduces tire efficiency and is responsible for heat build-up, is an essential property of tires, especially aircraft tires. A prominent example is the landing performance of an aircraft tire. During landing, the tire touches the ground with zero rotational speed under substantial load, thus creating massive friction between the tires and the ground. This combinations of high speed and high load results in a severe temperature increase within the tires. The temperature in the contact patch of the aircraft tire can reach up to 300°C.¹ This temperature is high enough to degrade the tire, which consists to a large portion of NR. High hysteresis can also have a negative impact on ultimate properties such as accelerated tread wear and decreased stress-strain properties. Another serious consequence is related to the chemical effects of temperature build-up on the properties of the final product: oxidation of polymer chains causing chain scission and a reduction of crosslink density resulting in softening of the rubber (as in natural rubber), or additional crosslink formation leading to rubber hardening as seen in styrene-butadiene rubber.

Several strategies are followed to minimize heat build-up and the deteriorating properties of rubber articles which are subjected to cyclic deformation. In the area of rubber mixing and compounding, the compound performance is not only determined by the right choice of the formulation components, but also by correct processing such as optimum parameter settings and addition sequence.

The polymer should be chosen to give low hysteresis at the temperature and frequency of interest.² Aircraft tire treads are generally made of blends of natural rubber (NR) and butadiene rubber (BR). The use of NR provides better mechanical strength such as superior tensile and tear properties, lower operating temperatures, reduced rolling resistance, excellent component-to-component adhesion, and good tire retreadability. A small portion of BR is added to improve the abrasion resistance.

Concerning the filler system, the attempts to minimize the hysteresis are decreasing the loading of fillers, decreasing the surface area of fillers or increasing the dispersion of fillers by prolonged mixing or more efficient mixing techniques. Carbon black (CB), in particular HAF blacks (high abrasion furnace), intermediate super-abrasion furnace (ISAF) and super abrasion furnace (SAF) types are commonly used in aircraft tire tread formulations to enhance abrasion resistance. Nowadays, silica becomes a strong alternative to CB fillers in tires, especially in passenger car tires. Studies revealed that silica provides a better balance in tire properties, in particular rolling resistance, heat build-up and wet grip, compared to CB.^{3,4} However, in aircraft tire treads, precipitated silica is used only in small amounts in combination with

CB. The substitution of low levels (5 to 10 phr) of carbon black by silica can enhance tear resistance, cut growth, and adhesion properties.⁵

Up to now, silica cannot replace CB entirely in the area of large tires or high-performance tires, where reinforcement and abrasion resistance become the essential properties. This is due to the fact that silica is less compatible with the polymers used for the treads of these tires, especially when NR is the primary polymer in the formulation. Silica is more difficult to disperse and can reduce the effectiveness of some components of the vulcanization system, resulting in reduced reinforcement and poorer performance than that of the CB counterpart.⁶ The use of silica with a high surface area can improve treadwear properties. However, a higher surface area means a higher number of silanol groups, which leads to an increase in filler-filler interaction. This increase in Payne effect leads to a higher hysteresis loss as well as a higher degree of adsorption of accelerators.⁷

The effect of zinc oxide (ZnO) and 1,3-diphenyl guanidine (DPG) in silica-filled compounds became the subject of investigations of many researchers.⁸⁻¹¹ ZnO can interact with the silica surface, resulting in a reduction of the reaction efficiency between silica and silane: the silanol groups on the silica surface are acidic of nature; therefore they can react with an alkali such as ZnO.⁸ DPG is known as a secondary accelerator which is generally used in combination with sulfenamide types of primary accelerators such as CBS in silica-filled compounds. DPG is capable of accelerating the silanization reaction, when this type of amine is added to a silica-silane compound.¹²

Considering the points mentioned above, this study aims to investigate the influence of the addition sequence of ZnO and DPG in CB-silica filled NR/BR compounds on the compound properties and hysteresis.

EXPERIMENTAL

MATERIALS

The rubbers used were Natural Rubber (Ribbed Smoked Sheet (RSS-1)), obtained from Weber & Schaefer GmbH & Co. KG, Germany; long chain branched-BR (LCB) BUNA Nd22EZ from Arlanxéo, Germany. The compounding ingredients were high structure carbon black N234 from Cabot, USA, Ultrasil 7005 and bis-(triethoxysilylpropyl)tetrasulfide (TESPT) from Evonik, Germany. Treated distillate aromatic extract oil (TDAE) was supplied from Hansen & Rosenthal, Germany. N-cyclohexyl-2-benzothiazole sulfenamide (CBS), 1,3-diphenylguanidine (DPG), 2,2,4-trimethyl-1,2-dihydroquinoline (TMQ), N-phenyl-para-phenylenediamine (6PPD), zinc oxide (ZnO), stearic acid and sulfur were of technical quality.

COMPOUND PREPARATION

The compound recipes are shown in Table I. The filler system used in this research is a hybrid of carbon black (CB) and silica (SI). The addition sequence of ZnO (Z) and DPG (D) is divided into first stage of mixing (I) and final stage (F). The amount of TESPT and DPG were calculated based on the CTAB specific surface area of silica, as suggested by Guy et al.¹³

TABLE I
COMPOUND FORMULATIONS

Mixing	Ingredients	CBSI-ZIDF	CBSI-ZIDI	CBSI-ZFDI	CBSI-ZFDF	
First stage	RSS-1	70	70	70	70	
	LCB-BR	30	30	30	30	
	N234	35	35	35	35	
	Ultrasil 7005	35	35	35	35	
	TESPT	3	3	3	3	
	ZnO	5	5	0	0	
	Stearic acid	3	3	3	3	
	6PPD	2	2	2	2	
	TMQ	1	1	1	1	
	TDAE	7.5	7.5	7.5	7.5	
	DPG	-	0.7	0.7	0	
	Final stage	Sulfur	1.5	1.5	1.5	1.5
		CBS	1	1	1	1
DPG		0.7	0	0	0.7	
ZnO		0	0	5	5	

Amount of TESPT and DPG were calculated according to the following equations:

$$\text{TESPT (phr)} = 0.00053 \times Q \times A \text{ and } \text{DPG (phr)} = 0.00012 \times Q \times A$$

Where Q is the amount of silica (phr) and A is the CTAB surface area of the silica (164m²/g)

Two-stage mixing was performed as shown in Table 2. NR is initially masticated to have a Mooney viscosity close to the Mooney viscosity of BR. The masticated NR and BR were mixed for 1 minute. Then silica, silane, half of the TDAE oil with or without DPG depending on the settings were added and mixed for 1 minute. After that, CB and other remaining ingredients with or without ZnO were added within 1 minute, and the rotor was adjusted in order to reach the targeted temperature for silanization. The ram was opened for about 1 minute to release ethanol produced in the silanization reaction. The temperature was maintained at 140°C for about 7 minutes to complete the silanization reaction. The compounds were then dumped, sheeted out on a two-roll mill and kept overnight prior to incorporation of sulfur, CBS with or without ZnO and DPG in an internal mixer at a temperature of 70°C and initial rotor speed of 50 rpm. After the masterbatch was mixed for 1 minute, the rotor speed was decreased to 30 rpm before curatives were added and mixed for 2 minutes (mins).

TABLE II
TWO-STEP MIXING PROCEDURE

	Mixing procedure	Time (mins)
Step 1: Internal mixer	- Mastication NR and BR	1
	- Addition of silica, silane, 1/2 TDAE oil, with/without DPG	1
	- Addition of CB and other remaining ingredients with/without ZnO	1
	- Ram sweep	1
	- Silanization reaction	7
Step 2: Internal mixer	- Masterbatch	1
	- Addition of curatives (sulfur and CBS) with/without DPG, ZnO	2

TESTING OF COMPOUND AND VULCANIZATE PROPERTIES

Mooney viscosity.– The compounds were tested for their Mooney viscosity by using a Mooney viscometer 2000VS (Alpha Technologies, USA) at 125°C with a large rotor for about 4 minutes with 1 minute of pre-heating according to ASTM D1646. The value is represented as ML(1+4)125°C. The measurement was performed at 125°C, because the initial viscosities of the compound were too high to be measured at a temperature of 100°C.

Cure behavior.– Scorch time (t_{s2}) and cure time (t_{90}) were tested using the rubber processing analyzer (RPA) at 150°C, with a frequency of 1.67 Hz and 6.98% strain. The cure rate index (CRI) was calculated according to Equation 1:

$$CRI = \frac{100}{t_{90} - t_{s2}} \quad \text{Equation 1}$$

Payne effect.– The complex modulus (G^*) of the compounds was measured using the RPA 2000 (Alpha Technologies, USA). A strain sweep test was done in the range of 0.56 to 100% strain at 0.5 Hz and 100°C. The difference of G^* at 0.56% and 100% strain was taken as a measure of filler-filler interaction.

Bound rubber content.– The uncured rubber compound (without curatives), approximately 0.2 gram, was cut and put into a metal cage and immersed in toluene at room temperature. The toluene was renewed every day. After three days, the sample was removed from the toluene and dried at 105°C for 24 hours. The sample was immersed again in the toluene for another three days at room temperature under either a normal or an ammonia atmosphere. The ammonia treatment was used to cleave the

physical linkage between rubber and filler, so that the chemically bound rubber can be determined. The sample was dried at 105°C for 24 hours. The bound rubber was calculated according to Equation 2:

$$\text{Bound rubber content} = \frac{m_r - m_f}{m_p} \times 100\% \quad \text{Equation 2}$$

where m_r is the dry weight of samples after toluene treatment either in a normal or ammonia treatment, m_f is the weight of the filler in the sample and m_p is the weight of the rubber in the specimen.

Crosslink density.— The samples were swollen in toluene at room temperature to an equilibrium swelling state and then removed from the solvent. The toluene on the surface of the sample was quickly blotted off with tissue paper. The samples were immediately weighed on an analytical balance and then dried in a vacuum oven. The volume fraction (V_r) of rubber in the swollen gel was calculated by Equation 3, and the crosslink density (X_c) was calculated by using the Flory-Rehner theory according to Equation 4:

$$V_r = \frac{m_1/\rho_1}{(m_1/\rho_1) + (m_2/\rho_2)} \quad \text{Equation 3}$$

where m_1 and m_2 are the weight of polymer and weight of solvent in the swollen sample at equilibrium swelling. ρ_1 is the density of un-swollen rubber vulcanizates and ρ_2 is the density of the solvent.

$$X_c = \frac{-(\ln(1-V_r) + V_r + \chi V_r^2)}{V_2(V_r^{1/3} - V_2/2)} \quad \text{Equation 4}$$

Where χ is the polymer-solvent interaction parameter (0.36)¹⁴, and V_2 is the molar volume of the solvent (106.3 cm³/mol).

Stress-strain properties.— All compounds were vulcanized at different cure times, ($t_{90}+2$) and ($t_{90} \times 4$) minutes (the time for tire vulcanization is usually four times longer than the cure time t_{90}), at 150°C. The sheets having a thickness of 2 mm were die-cut into dumbbells type 2 for the tensile test. The tests were done with a Zwick Roell Z1.0 machine using a crosshead speed of 500 mm/min according to ISO 37.

Hysteresis.— The compounds were cured to their ($t_{90}+2$) times at 150°C in the RPA and the hysteresis was measured in a frequency and a strain sweep. The first measurement was a frequency sweep in the range of 0.05 – 50 Hertz (Hz) at a fixed strain value of 10% and 200°C, the second test a strain sweep in the range of 0.1 – 100% strain at a fixed frequency of 0.5 Hz and 200°C.

Scanning electron microscopy–energy dispersive X-ray (SEM-EDX).— Vulcanized samples were extracted by acetone for 24 hours to remove non-rubber ingredients. The samples were then cut into small pieces. The cross-section surface was covered with a thin layer of gold to avoid electrostatic charging during the examination. SEM-EDX images were taken by a JEOL-JSM-T20.

RESULTS AND DISCUSSION

MOONEY VISCOSITY

Figure 1 shows the Mooney viscosity (MV) of the CB-silica filled NR/BR compounds with different addition sequences. Compounds containing ZnO from the masterbatch stage on show a lower MV compared to compounds with ZnO added in the last stage of mixing. When a high portion of NR is used, the zinc stearate, which forms from the reaction of ZnO and stearic acid, can influence the mastication process. Zinc stearate can act as peptizer, which is effective as a viscosity reducer in natural rubber, especially when carbon black is also present in rubber compound.¹⁵

The compounds are filled with carbon black and silica, and the soluble zinc can react with the silanol groups of the silica. This reaction competes with the function of ZnO as an activator for the accelerators. The mechanism here involves zinc ion attachment to silanol groups on the silica surface, reducing the silica network formation and resulting in a lower viscosity. The decrease of compound viscosity when ZnO is added in the masterbatch implies an improvement in silica dispersion.

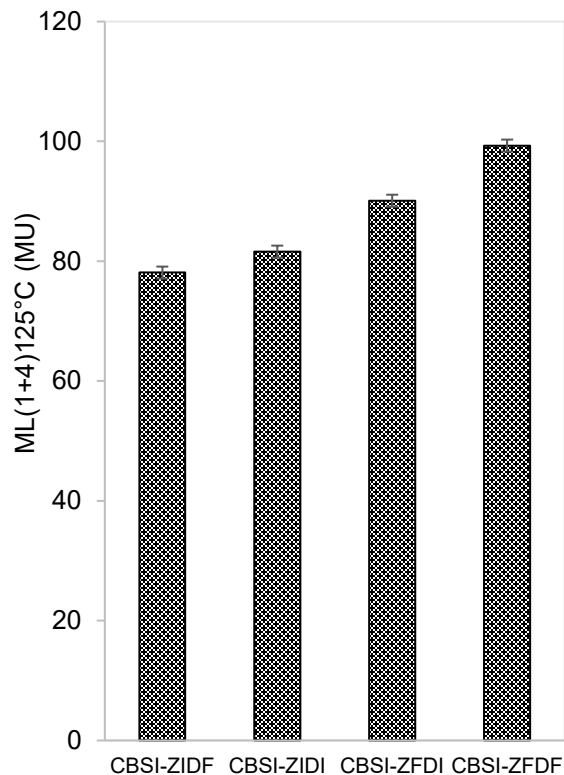


Figure 1.– Mooney viscosity of rubber compounds with different addition sequences of ZnO and DPG

CURE BEHAVIOR

Table III shows the curing characteristics of the various compounds with different ZnO and DPG addition sequences. ZnO is an inorganic compound which functions as an activator to speed up the vulcanization process. However, ZnO is difficult to disperse in the rubber matrix. Thus stearic acid is added to solubilize the zinc and set zinc ions free to form complexes with accelerators¹⁶. Addition of ZnO in the first stage of mixing allows the complete solubilization of ZnO by stearic acid. ZnO solubilized with stearic acid provides accelerator activation through the formation of intermediate accelerator complexes. Moreover, soluble zinc also reacts with silica silanols, and this reaction competes with the zinc activation function and leads to a reduction in the cure rate⁵. The DPG addition sequence does not influence the curing characteristics.

Figure 2 shows that no reversion is occurring when ZnO is added in the first stage of mixing. The presence of ZnO leads to a considerable decrease of the cure rate, which relates to the formation of a chelate complex between ZnO and the thiazole ring of the accelerator with the sulfur molecule attached to it. That complex may also have a thermo-stabilizing effect, thus preventing the destructive processes in the elastomers main chain or the crosslinked network already formed at the cure temperature¹⁷.

TABLE III
CURING CHARACTERISTICS OF COMPOUNDS

Characteristics	CBSI-ZIDF	CBSI-ZIDI	CBSI-ZFDI	CBSI-ZFDF
Scorch time, ts_2 (min)	4.2	4.9	3.3	2.7
Cure time, t_{90} (min)	11.0	12.7	8.4	7.3
Cure rate index, CRI (min^{-1})	14.7	12.8	19.6	21.7
Cure torque difference, MH – ML (dNm)	7.75	7.65	8.00	8.12

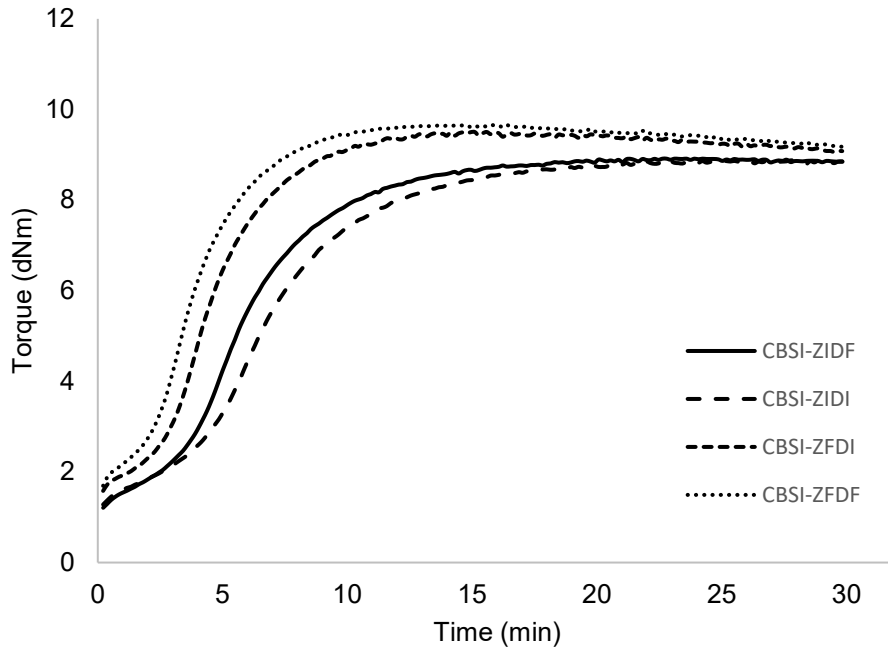


Figure 2.– Curing curves of rubber compounds at different ZnO and DPG addition sequences

PAYNE EFFECT AND FILLER-RUBBER INTERACTIONS

Figure 3 shows the Payne diagram of compounds at different ZnO and DPG addition sequences. The complex modulus G^* depends on the addition sequence of ZnO in these hybrid CB-silica filled rubber compounds. The complex modulus G^* of compounds, in which ZnO is added in the earlier stage of mixing, is lower in comparison to compounds with ZnO added in the final stage of mixing: ZnO can react well with stearic acid to produce soluble zinc ions, which interact with silica silanol moieties. The mechanism here involves zinc ion attachment to silica silanols, which reduces the silica network formation and results in lower viscosity⁵, thus improving silica dispersion.

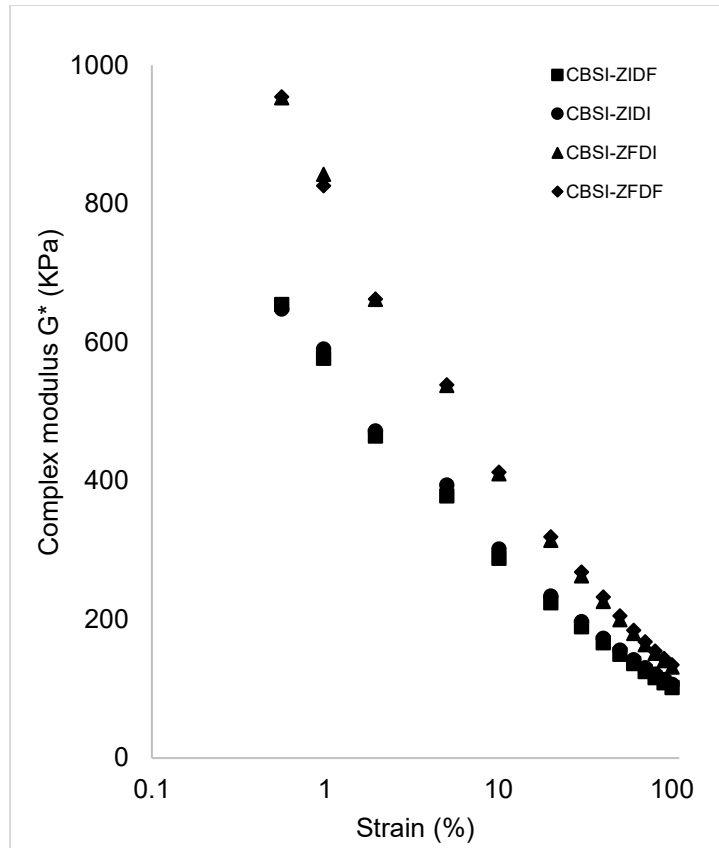


Figure 3.– Complex modulus versus strain of rubber compounds

The difference of G^* at low strain versus G^* at high strain indicates, how well the fillers disperse in the rubber matrix. A high Payne effect indicates strong filler-filler interactions, thus a low degree of dispersion. Compounds with ZnO added in the last stage of mixing show high G^* at low strain, which indicates high filler-filler interaction, and also slightly higher G^* at high strain. G^* at high strain can be correlated with filler-polymer interaction. The effect of DPG addition on the Payne effect is not significant in CB-silica filled compounds. This might be caused by the long silanization time of 7 minutes, during which a complete silanization reaction has been reached. Therefore the effect of DPG as silanization booster cannot be seen anymore.

Next to the DPG addition sequence, the silanization reaction time was varied from 3 to 7 minutes to prove, that DPG is acting as a silanization booster. Figure 4a shows that at short silanization times, thus when the silanization reaction is not completed, the addition of DPG together with silica in the first stage of mixing can indeed promote the silanization reaction resulting in lower filler-filler interaction compared to the addition of DPG in the final step. However, when the silanization was complete, both compounds show the same Payne effect regardless of the DPG addition, as shown in Figure 4b.

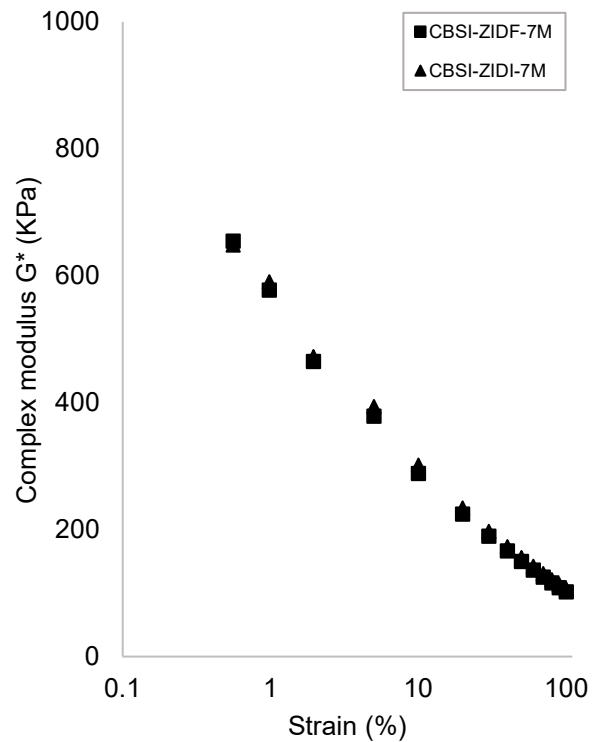
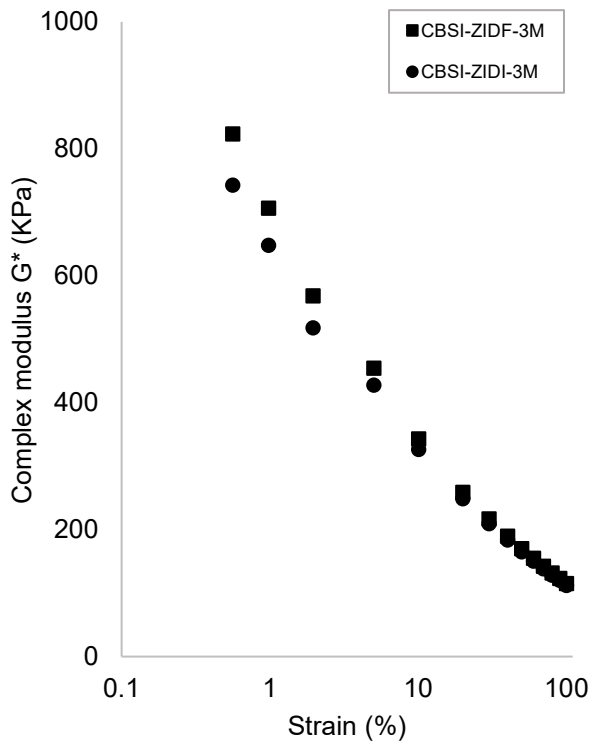


Figure 4a.– Payne effect of different DPG addition sequences at 3 minutes silanization time

Figure 4b.– Payne effect of different DPG addition sequences at 7 minutes silanization time

Bound rubber measurements were performed to assess whether G^* at high strain correlates with filler-polymer interaction. The addition of ZnO in the final stage of mixing increases filler-polymer interaction, as depicted in Figure 5. When ZnO is added in the masterbatch, ZnO can interact with silanol groups of silica, thus interfering with the silane bonding to the silica surface during silanization. By adding ZnO in the final stage, the silanization reaction efficiency increases. The interaction between alkoxy groups of TESPT and silanol groups on the silica surface during the mixing process leads to a reduced hydrophilicity of the silica surface and thus, improved rubber-filler interaction.¹⁸ The results of bound rubber measurements are consistent with the values of G^* at high strain from Payne measurements.

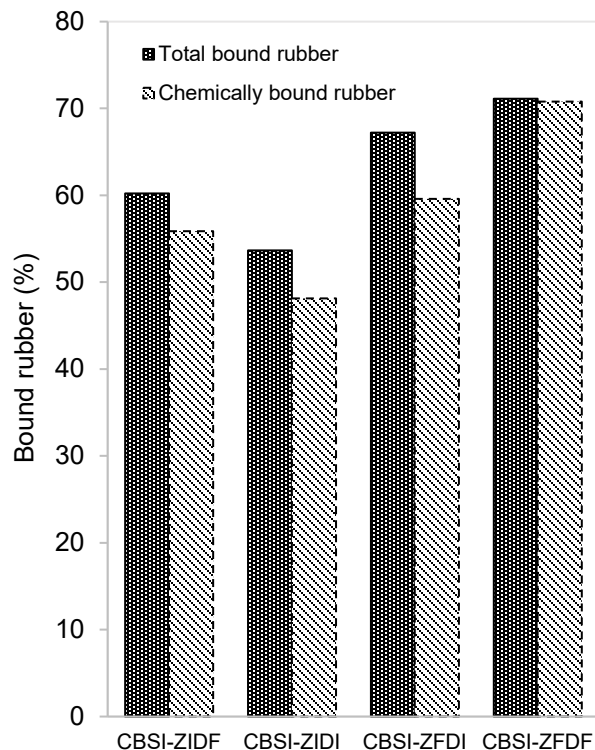


Figure 5.– Bound rubber content of compounds at different ZnO and DPG addition sequences

CROSSLINK DENSITY

Figure 6 shows the value of crosslink density measured by equilibrium swelling of the rubber compounds cured at standard vulcanization time ($t_{90}+2$) minutes, as well as at extended vulcanization times ($t_{90} \times 4$) minutes. There is no significant effect of ZnO and DPG addition sequence on crosslink density at ($t_{90}+2$) minutes. The vulcanizates have similar levels of crosslink networks at various mixing sequences. However, the prolonged cure time, ($t_{90} \times 4$) minutes for the vulcanizates, in which ZnO was added in the final stage of mixing, show a higher reduction of crosslink density compared to compounds containing ZnO from the first stage of mixing. The results are in line with the curing curve as shown in Figure 2, in which the compounds with ZnO added in the last stage of mixing show high reversion.

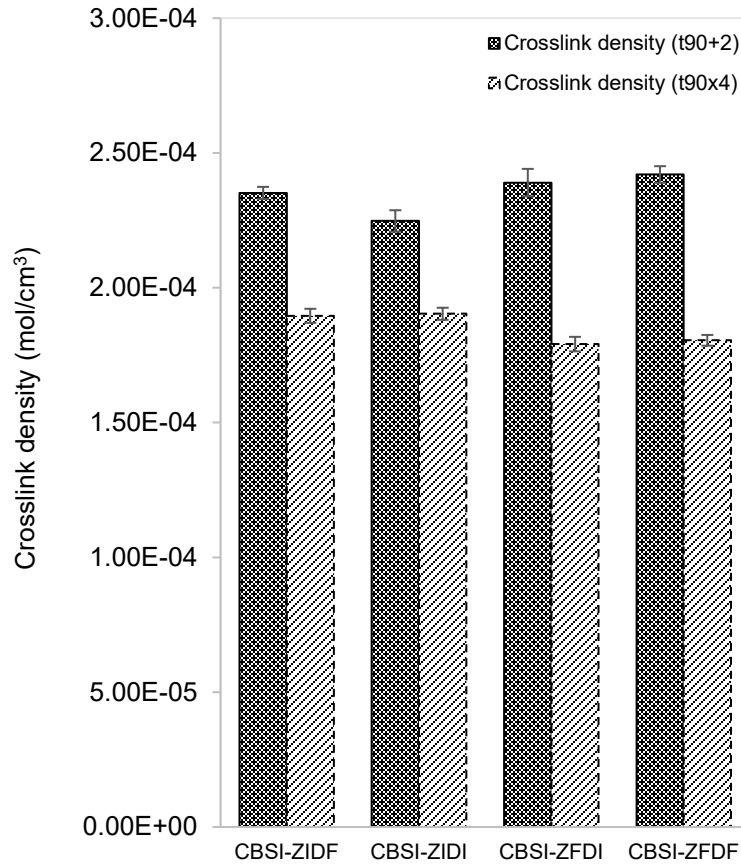


Figure 6.– Crosslink density of rubber compounds at different addition sequence of ZnO and DPG

STRESS-STRAIN PROPERTIES

Tensile strength and modulus 300% can be used as indications of reinforcement. Those properties depend on the filler reinforcement as well as the polymer network (crosslinks) created during vulcanization. Reinforcement requires good dispersion of the filler (low filler-filler interaction). During mixing, the filler agglomerates become distributed, the polymer is incorporated into the void spaces of the latter, and they are broken down into distinct aggregates. Occluded rubber is polymer chains trapped in the voids of the filler structure. Occluded rubber increases the effective filler volume and can only be destroyed at increasing stress. Bound rubber is an immobilized polymer layer derived from the polymer chains adsorbed onto the filler surface, which cannot be removed easily. Another contribution of the polymer to reinforcement are entanglements and the degree of crosslinking formed during vulcanization.

Figure 7 shows the tensile strength of the investigated vulcanizates obtained for different cure times (t_{90+2} and t_{90x4}). The ZnO and DPG addition sequence has almost no effect on tensile strength at these different cure times. However, the ZnO addition sequence does affect M300%: Compounds containing a high bound rubber content show higher M300% values compared to compounds with lower bound rubber contents. However, at long vulcanization times, compounds containing ZnO added in the last stage of mixing show a slightly higher reduction of M300% compared to compounds with ZnO added in the first stage of mixing. These results correlate with the Payne effect diagrams in Figure 3 in which the difference in complex modulus at low and high strain indicates worse dispersion, and the cure curves which show reversion as an indication of polymer or crosslink breakdown and high crosslink density reduction (Figure 2).

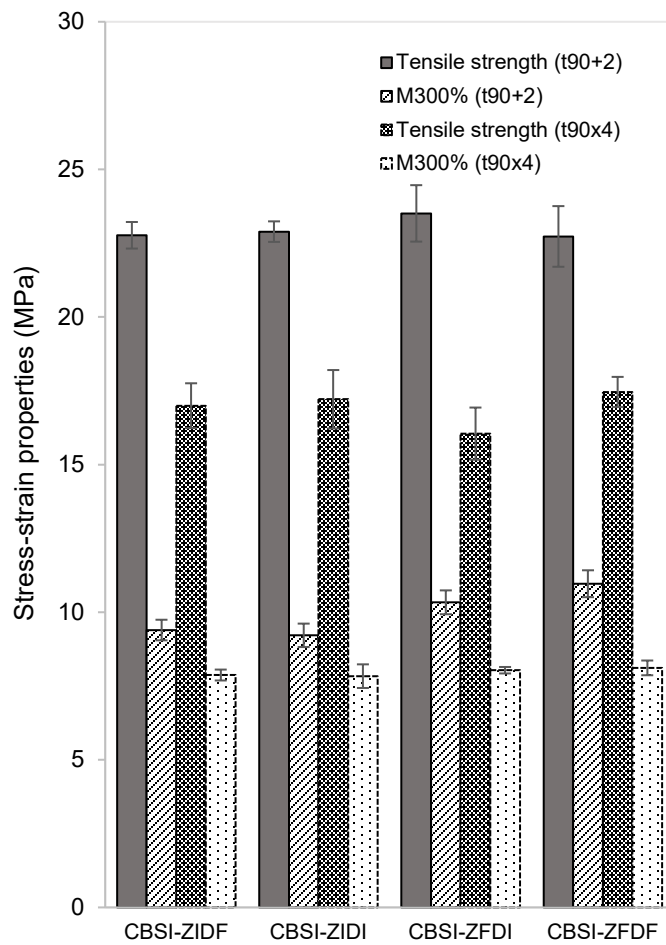


Figure 7.- Stress-strain properties of rubber compounds

HYSTERESIS

The amount of heat generated is dependent on the mode of deformation. If stress is plotted against strain, for one cycle of deformation, the hysteresis loop (H) can be calculated with Equation 5²:

$$H = \left(\frac{\pi}{4}\right) \times \left(\frac{DSA}{100}\right)^2 \times G' \tan \delta \quad \text{Equation 5}$$

where DSA is the double or peak-to-peak strain amplitude (the maximum strain in and out of phase) in % of the undeformed dimension, and G' is the storage modulus. When the rubber is subjected to constant strain deformation, the hysteresis is proportional to the $G' \tan \delta$ or G'' (loss modulus). When the rubber experiences constant stress deformation, the hysteresis is proportional to the loss compliance (J''), see Equation 6:

$$J'' = \frac{G'}{G'^2} \approx \frac{\tan \delta}{G'} \quad \text{Equation 6}$$

Deformation of a tread can be resolved into constant strain (bending) and constant stress (compression). Therefore, the contribution to heat build-up in a tire is (a) G'' , the out of phase modulus and (b) $\tan \delta/G'$.^{19, 20}

The effect of ZnO and DPG addition sequence on hysteresis is investigated, and the results are shown in Figure 8 for the hysteresis measured by the loss modulus G'' and loss compliance J'' using a frequency sweep at 10% strain deformation. The RPA frequency sweep test provides useful information on the viscoelastic behavior of the tire running at different speeds. It can be seen from Figure 8, that the ZnO and DPG addition sequence does not have a significant effect on the dynamic properties as measured by G'' and J'' . The hysteresis of rubber vulcanizates is influenced by many factors such as type of polymers, filler dispersion, filler-polymer interaction and crosslink density. As seen in Figure 3, a clear difference in Payne effect is observed; however, the lower Payne effect values only have a slight influence on J'' . In this system, the low Payne effect does not lead to high filler-polymer interactions. When ZnO is added in the first stage of mixing together with silica and TESPT, Zn ions can interact with the silica surface, thus covering more silica surface and resulting in a low Payne effect, as explained above. Zinc ions thus block the access of TESPT and inhibits bonding with silica, resulting in a low amount of chemically bound rubber as a consequence of insufficient silanization. Moreover, the different addition sequences of ZnO and DPG result in a similar degree of crosslinking. The three-dimensional network restricts the mobility of the polymer chains. The increase of frequency “freezes” the chain movements, and a stiffer behavior is observed (G'' increases). This combination of properties result in an insignificant difference in hysteresis (G'' and J'').

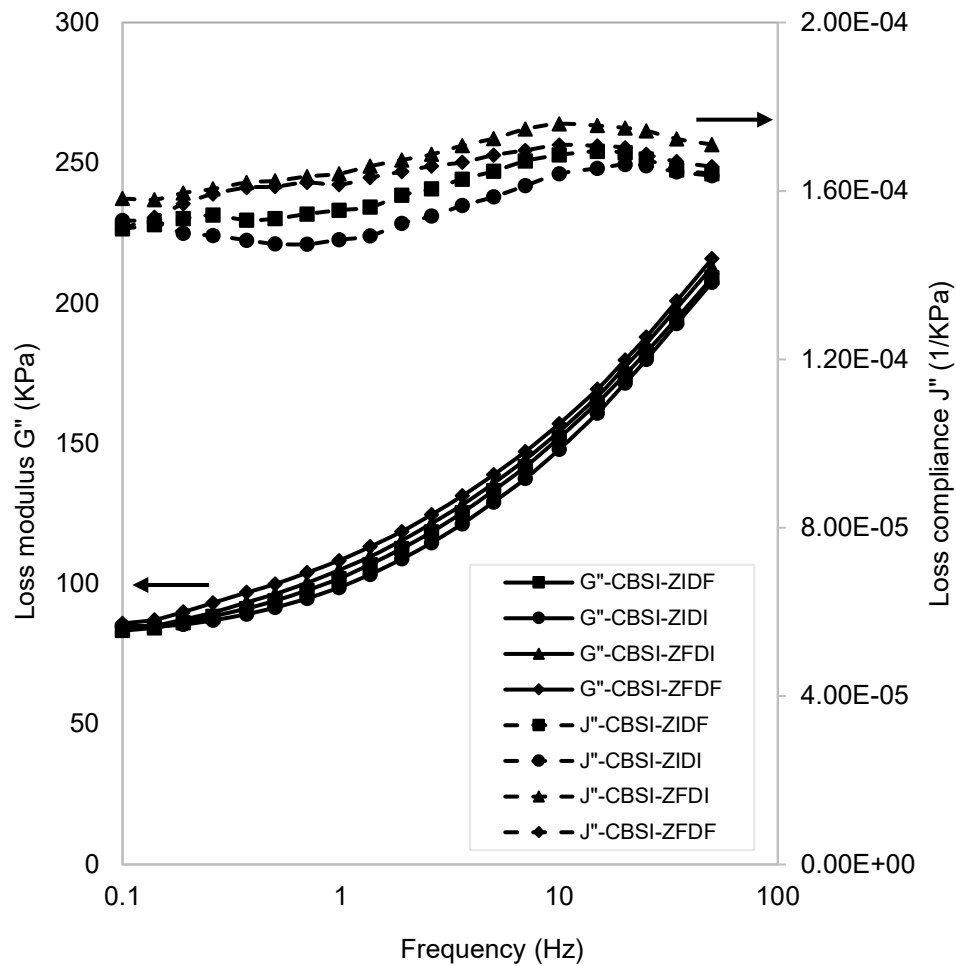


Figure 8.– G'' and J'' versus frequency as a measurement of hysteresis

Figure 9 shows the effect of the ZnO and DPG addition sequence on the hysteresis as measured by loss modulus G'' and loss compliance J'' in a different mode: in a strain sweep. The RPA strain sweep test provides useful information on the viscoelastic behavior of the tire running at different strain (bending) deformations of the tire. The addition sequence of ZnO and DPG does not have any influence on G'' and J'' with increasing strain. This result is in line with the measurement of energy dissipation as hysteresis loop in a stress-strain diagram (see Figure 10) for one cycle of deformation: all compounds show similar energy loss (see Table IV).

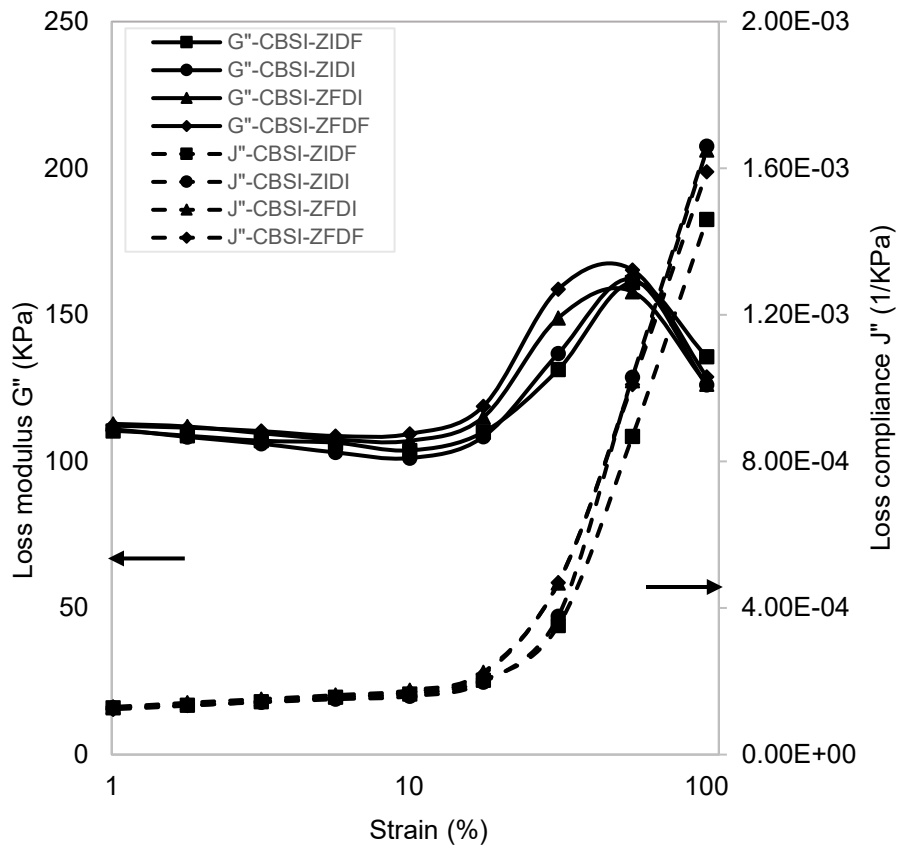


Figure 9.– G'' and J'' versus strain as a measurement of hysteresis

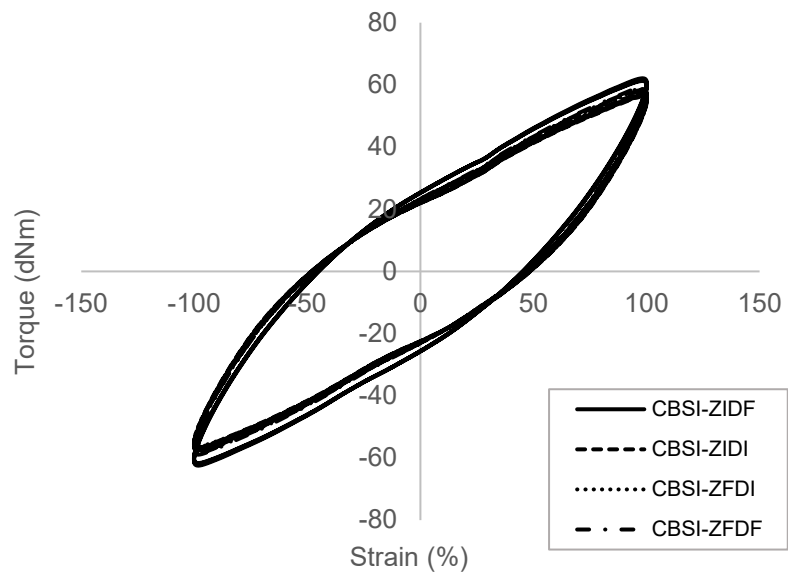


Figure 10.– Stress against strain for one cycle of deformation

TABLE IV
ENERGY DISSIPATION OF COMPOUNDS

Compound	CBSI-ZIDF	CBSI-ZIDI	CBSI-ZFDI	CBSI-ZFDF
Energy dissipation (J)	7.27	7.28	7.43	7.83

SEM-EDX IMAGES OF SILICA AND ZINC OXIDE

The SEM-EDX study for silica dispersion is shown in Figure 11. The silica dispersion is improved when ZnO is added in the first stage of mixing. This evidence is in line with the results of the Payne effect measurements in Figure 3, in which compounds with ZnO added in the first stage of mixing show a lower Payne effect compared to compounds with ZnO added in the last stage of mixing. The dispersion of the silica in the rubber matrix can be arranged as follows:

$$\text{CBSI-ZIDF} \approx \text{CBSI-ZIDI} > \text{CBSI-ZFDI} > \text{CBSI-ZFDF}$$

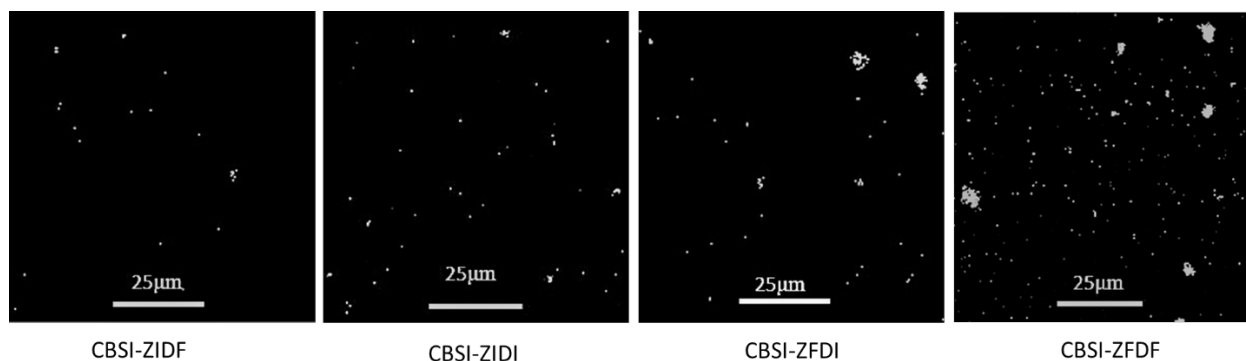


Figure 11.– SEM-EDX images for silica dispersion in rubber compounds at different ZnO and DPG addition sequences

Figure 12 shows the ZnO dispersion images from SEM-EDX. It is expected that ZnO reacts with stearic acid when it is added in the first stage of mixing, resulting in better solubility of ZnO in the rubber matrix. From the pictures it is obvious that compounds with ZnO added in the last stage show more heterogeneous Zn-particles in the rubber matrix. While the compounds with ZnO added in the first stage of mixing show a relatively small size of Zn particles.

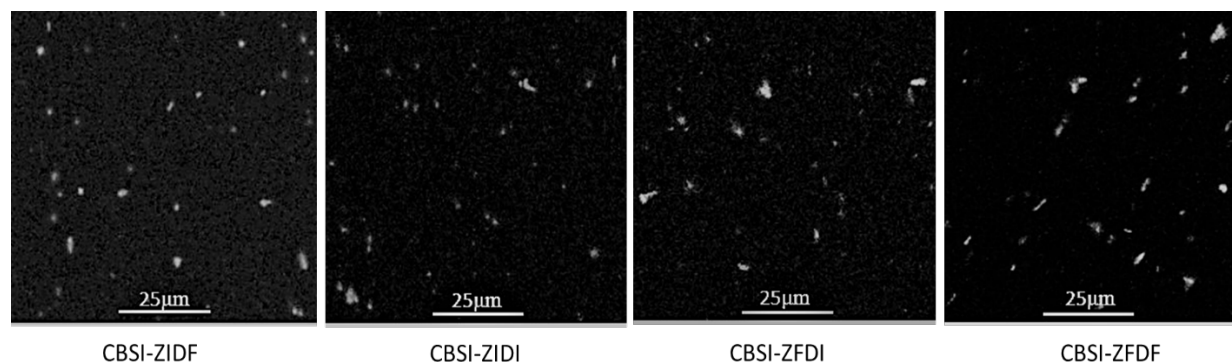


Figure 12.– SEM-EDX images for ZnO dispersion in rubber compounds at different ZnO and DPG addition sequences

CONCLUSIONS

Hybrid CB and silica filled NR/BR compounds were investigated with focus on the effect of the ZnO and DPG addition sequence on the material properties with specific interest on the hysteresis. From the study it can be concluded, that the ZnO addition sequence has a strong influence, while the DPG addition sequence has almost no effect on the properties of hybrid CB-silica filled rubber compounds. Addition of ZnO in the first stage of mixing decreases Mooney viscosity and results in better dispersion as indicated by lower filler-filler interaction (Payne effect) and SEM-EDX. Although the cure rate of the compounds decreased compared to compounds in which ZnO was added in the final stage of mixing, compounds with ZnO added in the masterbatch stage are more resistant to polymer degradation (plateau curing curve). This is expressed in a small change of crosslink density and M300% when extending the cure time from $t_{90}+2$ to $t_{90} \times 4$. However, compounds with ZnO added in the last stage of mixing show high bound rubber contents as a result of a better silanization efficiency. High filler-polymer interaction increases stress-strain properties. However, due to the reversion, the compounds experience a high reduction of crosslink density, thus decreased M300% at long vulcanization times. In the case of the dynamic properties responsible for the hysteresis, the addition sequence of ZnO and DPG does not have any effect on G'' and J'' at various frequencies and strains. Considering all properties above, the addition of ZnO in the first stage of mixing in hybrid silica-carbon black filled NR/BR is more suitable for aircraft tire tread applications.

REFERENCES

1. Alroqi, A.A., et al., *J. Aircraft*, 54, 926 (2017).
2. Medalia, A.I., RUBBER CHEM. TECHNOL., 64, 481 (1990).
3. Luginland, H.D. and Niedermeier, W., *Rubber World*, 228, 34 (2003).
4. Schwaiger, B. and Blume, A., *Rubber World*, 222, 32 (2000).
5. Hewitt, N. Chapter 2: Compounding Precipitated Silica in Natural Rubber in "Compounding Precipitated Silica in Elastomers", William Andrew Publishing, New York, 2007.
6. Chakraborty, S., et al., *Rubber World*, 248, 37 (2013).
7. Meon, W., et al. Chapter 7: Silica and Silanes, in "Rubber Compounding: Chemistry and Applications", B. Rogers ed., Marcel Decker, 2004.
8. Reuvekamp, L.A.E.M., *Reactive Mixing of Silica and Rubber for Tyres and Engine Mounts: Influence of Dispersion Morphology on Dynamic Mechanical Properties*, PhD. Thesis, Elastomer Technology and Engineering, University of Twente, The Netherlands (2003).
9. Kim, I.J., et al., *J. Applied Polymer Science*, 117, 1535 (2010).
10. Maghami, S., *Silica-Filled Tire Tread Compounds: An Investigation Into the Viscoelastic Properties of the Rubber Compounds and Their Relation to Tire Performance*, PhD. Thesis, Elastomer Technology and Engineering, University of Twente, The Netherlands (2016).
11. Mihara, S., *Reactive Processing of Silica-Reinforced Tire Rubber: New Insight into The Time- And Temperature-Dependence of Silica Rubber Interaction* PhD. Thesis, Elastomer Technology and Engineering, University of Twente, The Netherlands (2009).
12. Penot, C., US6951897B2 (to Michelin Recherche et Technique S.A), Oct. 4 (2005).
13. Guy, L., et al., *Kaut. Gummi Kunstst.*, 62, 383 (2009).
14. Allen, P.W. and Bristow, G.M., *J. Applied Polymer Science*, 3, 603 (1963).
15. Further Developments on Metal Soaps as Processing Promoter for The Rubber Industry Available online: <https://static1.squarespace.com/static/developmentsonmetalsoaps.pdf> (accessed on Sept. 5, 2019).
16. Heideman, G., *Reduced Zinc Oxide Levels in Sulphur Vulcanisation of Rubber Compounds; Mechanistic Aspects of the Role of Activators and Multifunctional Additives*, PhD Thesis, Elastomer Technology and Engineering, University of Twente, The Netherlands (2004).
17. Todorova, N., et al., *J. Chemical Technology and Metallurgy*, 49, 213 (2014).
18. Pattanawanidchai, S., et al., *Polymer Engineering and Sciences*, 59, 42 (2019).
19. Payne, A.R. and Whittaker, R.E., *J. Applied Polymer Science*, 16, 1191 (1972).
20. Collin, J.M., et al., RUBBER CHEM. TECHNOL., 38, 400 (1965).